HAL
open science

Removable air-cathode to overcome cathode biofouling in microbial fuel cells

Manon Oliot, Luc Etcheverry, Alain Bergel

To cite this version:

Manon Oliot, Luc Etcheverry, Alain Bergel. Removable air-cathode to overcome cathode biofouling in microbial fuel cells. Bioresource Technology, 2016, 221, pp.691-696. 10.1016/j.biortech.2016.09.095 . hal-02134859

HAL Id: hal-02134859

https://hal.science/hal-02134859v1

Submitted on 20 May 2019

HAL is a multi-disciplinary open access archive for the deposit and dissemination of scientific research documents, whether they are published or not. The documents may come from teaching and research institutions in France or abroad, or from public or private research centers.

L'archive ouverte pluridisciplinaire **HAL**, est destinée au dépôt et à la diffusion de documents scientifiques de niveau recherche, publiés ou non, émanant des établissements d'enseignement et de recherche français ou étrangers, des laboratoires publics ou privés.

Open Archive Toulouse Archive Ouverte (OATAO)

OATAO is an open access repository that collects the work of some Toulouse researchers and makes it freely available over the web where possible.

This is an author's version published in: http://oatao.univ-toulouse.fr/20490

Official URL: https://doi.org/10.1016/j.biortech.2016.09.095

To cite this version:

Oliot, Manon and Etcheverry, Luc and Bergel, Alain Removable air-cathode to overcome cathode biofouling in microbial fuel cells. (2016) Bioresource Technology, 221. 691-696. ISSN 0960-8524

Any correspondence concerning this service should be sent to the repository administrator:
tech-oatao@listes-diff.inp-toulouse.fr

Removable air-cathode to overcome cathode biofouling in microbial fuel cells

Manon Oliot *, Luc Etcheverry, Alain Bergel

Laboratoire de Génie Chimique CNRS – Université de Toulouse (INPT), 4 allée Emile Monso, 31432 Toulouse, France

HIGHLIGHTS

- An innovative MFC design allowed the air-cathode to be removed and replaced.
- Replacing the air-cathode immediately boosted power density from 0.7 to 1.96 W/m^2.
- Initial biofouling of air-cathodes may be a widespread cause of underperformance.
- Air-cathode replacement was modelled numerically.

Keywords:
Bioelectrochemical system
Bioanode
Reactor design
Numerical modelling

ABSTRACT

An innovative microbial fuel cell (MFC) design is described, which allows the air-cathode to be replaced easily without draining the electrolyte. MFCs equipped with 9-cm^2 or 50-cm^2 bioanodes provided 0.6 and 0.7 W/m^2 (referred to the cathode surface area) and were boosted to 1.25 and 1.96 W/m^2, respectively, when the initial air-cathode was replaced by a new one. These results validate the practical interest of removable air-cathodes and evidence the importance of the cathode biofouling that takes place during the MFC starting phase. As this biofouling is compensated by the concomitant improvement of the bioanodes it cannot be detected on the power curves and may be a widespread cause of performance underestimation.

1. Introduction

Microbial fuel cells (MFCs) can convert the chemical energy contained in a large variety of organic compounds into electrical energy. Such systems are composed of a microbial anode, which catalyses the oxidation of organic matter and is associated with a cathode, which is most often an abiotic air-cathode that ensures oxygen reduction (Ahn et al., 2014; Ye et al., 2016). Considerable advances have been made in bioanodes (Rimboud et al., 2014) but, in contrast, the oxygen-reducing cathodes remain a major rate-limiting step. There are several reasons for this, including the modest solubility of oxygen in water, the poor efficiency of O_2-reduction catalysts at the neutral pH values that are required to grow microbial anodes and, particularly in the case of abiotic air-cathodes, sensitivity to fouling.

When implemented in an MFC, the side of the air-cathode in contact with the electrolyte is exposed to a solution rich in microorganisms, organic compounds and salts. Bacteria colonize the cathode surface, forming a biofilm (Ma et al., 2014; Rismani-Yazdi et al., 2008), which may hinder the transport of the hydroxide ions away from the electrode and consequently enhance alkalinization in the vicinity of the cathode surface (Ma et al., 2014; Yuan et al., 2013):

$$O_2 + 2\ H_2O + 4e^- \rightarrow 4\ OH^- \quad (1)$$

Local alkalinization is detrimental to the oxygen reduction reaction from the point of view of thermodynamics and it also contributes to the deactivation of the cathode via the precipitation of cations in the form of hydroxides and scale (Tlili et al., 2003), particularly Ca^{2+} or Mg^{2+}, which are commonly present in the MFC electrolytes (Santoro et al., 2013; Ma et al., 2014; Santini et al., 2015). Various solutions have been proposed to mitigate air-cathode biofouling (Chatterjee and Ghangrekar, 2014; Li et al., 2014; Liu et al., 2015) including a separator to protect the cathode

* Corresponding author.
E-mail address: manon.oliot@ensiacet.fr (M. Oliot).

http://dx.doi.org/10.1016/j.biortech.2016.09.095

surface from organic compounds (Song et al., 2015), antimicrobial coating to mitigate biofilm formation (Pu et al., 2014), or modification of the cathode composition (Wang et al., 2014; Zhou et al., 2016).

The solutions envisioned so far are one-shot options, i.e. they are designed at the beginning of the MFC's life and do not allow intervention during MFC operation. Once the air-cathode has been placed in the system, it cannot be removed without draining the anolyte because the air-cathode is generally part of the cell wall. With common MFC architecture, removing the air-cathode results in the loss of a large part of the electrolyte, which could severely disturb the bioanode, through exposure to ambient air, for instance.

The present study describes an innovative MFC design, which allows the air-cathode to be replaced easily. The fouled air-cathode can thus be cleaned or replaced without changing the electrolyte and without altering the bioanode. Surprisingly, using this new device to change the air-cathode in the course of MFC operation revealed the unsuspected magnitude of initial biofouling, which may have been a widespread cause of underestimation of MFC performance up to now.

2. Materials and methods

2.1. Reactor design

The reactor was designed so that three distinct operations could be carried out:

- Firstly, formation of the bioanode under controlled potential (chronoamperometry). The reactor was set in a standing position, the anode and the reference electrode were fixed on the reactor side and the auxiliary electrode was maintained on the top (Fig. 1A).
- Secondly, use of the reactor as an MFC. Once the bioanode formed in chronoamperometry was mature, the auxiliary electrode was removed and replaced by an abiotic air-cathode on the top. The reactor was then tilted to the side in order to bring the air-cathode fully into contact with the solution. The reactor was held in this lying position during MFC operation (Fig. 1B).
- Thirdly, when the efficiency of the air-cathode fell, return of the MFC to the standing position so as to change the air-cathode without draining the electrolyte and without exposing the bioanode to air or to any other disturbance. After the cathode had been changed, the reactor was tilted into the lying position again to continue MFC operation.

The reactor had a volume of 1.8 L. All experiments were carried out in a heat chamber at 40 °C. The bioanodes were designed from compost leachate with acetate as the substrate:

$$CH_3COO^- + 4H_2O \rightarrow 2HCO_3^- + 9H^+ + 8e^- \quad (2)$$

2.2. Bioanode formation under chronoamperometry (CA)

Bioanodes were formed using a 3-electrode set-up with the reactor in the standing position (Fig. 1A). Carbon cloth (PaxiTech, Grenoble, France) was used as the anode support (working electrode). Electrodes with two different geometrical surface areas were compared: 9 cm^2 (3 cm × 3 cm) and 50 cm^2 (5 cm × 10 cm). Both electrodes had a thickness of 1 mm, so the total active surface areas used for current density calculations were 19.2 and 103 cm^2, respectively, including the edge area. A platinum grid was used as the auxiliary electrode and a saturated calomel electrode as the reference (SCE, potential +0.242 V/SHE). The working electrode was polarized at −0.2 V/SCE using a VSP potentiostat (Bio-Logic SA, France).

The bioanodes were formed under CA for 20 days in compost leachate, prepared as described elsewhere (Parot et al., 2008; Cercado et al., 2013) and supplemented with acetate. Acetate concentration was maintained at 20 mM by periodic measurements (Megazyme K-Acetak kit, Ireland) and additions. Once mature bioanodes were producing around 10 $A.m^{-2}$, the solution was replaced by a fresh synthetic medium (bicarbonate buffer 50 mM at pH 9, macronutrients 10 $mL.L^{-1}$, micronutrients 1 $mL.L^{-1}$, vitamins 1 $mL.L^{-1}$, KCl 4.5 $g.L^{-1}$ and $NaH_2PO_4{\cdot}H_2O$ 2.4 $g.L^{-1}$; pH adjusted to 7.0) and the bioanodes were polarized for 10 additional days. When they were delivering around 10 $A.m^{-2}$, the reactor was equipped with an air-cathode.

2.3. MFC operation

The air-cathode (PaxiTech, Grenoble, France) was assembled with a current collector (stainless steel) on a PVC screw cap designed with a central hole 4.5 cm in diameter, which resulted in an area of 15.9 cm^2 of the air-cathode being exposed to the electrolyte. The cap was screwed onto the top of the reactor and the reactor was tilted into the lying position (Fig. 1B). In this position, the anode and reference were on the top and the air-cathode was in a vertical position on the reactor side. During MFC operation, acetate concentration was maintained at 20 mM by periodic measurements and additions. Power curves were recorded periodically, using a variable external resistance ranging from 0 to 33,000 Ω. A high-impedance voltmeter (Keithley, 2000 multimeter, USA), in

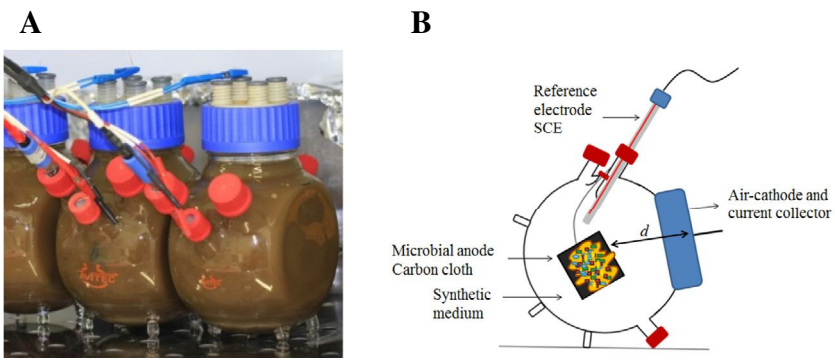

Fig. 1. Reactor design. (A) Photograph of reactors in standing position during formation of bioanodes under chronoamperometry (CA) with compost leachate as electrolyte. (B) Scheme of the reactor in lying position during MFC operation. The counter electrode was replaced by an air-cathode fixed on the blue screw cap with the current collector. (For interpretation of the references to colour in this figure legend, the reader is referred to the web version of this article.)

derivation of the resistance, measured the cell voltage and a second voltmeter measured the anode and cathode potentials versus the SCE reference. MFCs produced power continuously through an electrical resistance, which was adapted, generally in the range 30–100 Ω, so that the MFCs could operate close to their maximum power. Power densities were expressed relative to the 15.9 cm^2 air-cathode surface area.

2.4. Numerical modelling

The numerical model was based on the secondary distribution of the electrostatic potential inside the cell, described by the Laplace equation. The theoretical basis and the numerical procedure have been detailed previously for the case of a microbial electrolysis cell (Lacroix et al., 2014). They were identical here for an MFC. The model was fed with the cell geometry, the conductivity of the electrolyte and the experimental kinetics (i-E curves) of the bioanode and the air-cathode (details in Supplementary Data). The numerical model was solved with the Comsol Multiphysics software package equipped with the "Electrochemistry" module.

On the basis of the experimental kinetics, the reactor geometry and the ionic conductivity of the medium, the model gave the distribution of the electrostatic potential, the current distribution on the electrode surfaces and, finally, the performance that the MFC electrodes could display. It is important to note that no parameter was numerically adjusted.

3. Results and discussion

3.1. MFC operation

Bioanodes were formed under chronoamperometry (CA) at −0.2 V/SCE in compost leachate for 20 days. The electrolyte was then replaced by a synthetic medium, without inoculum, for 10 additional days of CA, before switching to MFC operation. The aim of this procedure was to work in a clean medium and thus to avoid as much (bio)fouling of the air-cathode surface as possible. Four MFCs were run in identical conditions, two with bioanodes of 9 cm^2 geometrical area and two with bioanodes of 50 cm^2 geometrical area.

At day 0, the two MFCs equipped with 9-cm^2 bioanodes gave similar power curves and similar maximum power, around 1 mW (Fig. 2A and B). The power curves did not display a symmetrical bell shape, the right parts (low resistance, high current) being close to vertical. As already explained (Pocaznoi et al., 2012), this behaviour identified the rate-liming effect of the bioanode. In contrast, the two 50-cm^2 bioanodes led to symmetrical bell-shaped power curves (Fig. 3A and B). Because of their large surface area in comparison to the air-cathodes of 15.9 cm^2, the 50-cm^2 bioanodes did not limit the MFC performance. The rate-limiting effect of the 9-cm^2 bioanodes was confirmed by current-potential (i-E) curves (Fig. 2C), which showed a maximum current plateau starting at around 4.8 mA. For resistances lower than 100 Ω, the bioanodes were not able to produce more than the 4.8 mA. At the same time, the air-cathodes gave a conventional i-E curves of oxygen reduction (Fig. 2C).

At day 10, the i-E curve of each bioanode showed improved kinetics (Figs. 2C and 3C). The 9-cm^2 bioanodes were able to provide up to 6.8 mA, and all the i-E curves were shifted by around 70 mV towards negative potentials in comparison to the i-E curves recorded at day 0. The open circuit potential (OCP) decreased by 50 ± 14 mV (average for the 4 bioanodes).

In contrast, the air-cathodes lost a considerable proportion of their efficiency during the same period (Fig. 2C). The cathode OCPs decreased by 212 ± 45 mV (average for the 4 cathodes) and the i-E curves as a whole were shifted towards negative potentials. Such a performance decrease is usually attributed to biofouling of the air-cathode surface (Ma et al., 2014; Rismani-Yazdi et al., 2008). Here, an extensive slimy film, including a thick brown deposit, was visible with the naked eye on the side of the air-cathode in contact with the solution (Fig. 1 in Supplementary Data). Epifluorescence microscopy confirmed the presence of microorganisms on the surface, whereas no microorganisms were initially present on the surface of the clean air-cathode (Fig. 1 in Supplementary Data).

The behaviour of the MFC during the initial period of operation was consequently the result of two opposite phenomena:

- the improvement in the bioanode kinetics,
- the decrease in the air-cathode kinetics because of biofouling.

These two phenomena were confirmed by the four MFCs. The behaviour of each MFC is consequently controlled by the ratio of their strengths. When the air-cathode deterioration is greater than the bioanode improvement, the maximum power can decrease significantly, as was the case here with an MFC that produced 1 mW initially and 0.47 mW after 10 days (Fig. 2B). When the two phenomena approximately cancel each other out, the MFC performance appears nicely stable, as was the case here for three MFCs. An MFC equipped with a 9-cm^2 bioanode produced 0.9 to 0.76 mW during the first 10 day period (Fig. 2A), the two MFCs equipped with 50-cm^2 bioanodes delivered fairly stable power, around 1.2 mW.

After day 10, the three MFCs that continued to operate without change showed a stabilization of the cathode i-E curve. Thus, biofouling had a rapid detrimental effect on the clean air-cathodes and then led to stable degraded kinetics.

At day 10, the MFC equipped with a 9-cm^2 bioanode that showed the lowest performance had its air-cathode replaced by a new one. The design of the reactor allowed this operation to be achieved easily without draining the electrolyte or disturbing the bioanode. Maximum power immediately increased from 0.46 to 1.99 mW (Fig. 2B). The kinetics curves (Fig. 2C) showed that, as expected, the replacement of the air-cathode did not affect the bioanode. This confirmed the suitability of the reactor design and of the cathode removal procedure. The increase in MFC performance is explained by the efficiency of the new air-cathode, which showed an OCP of 0.2 V/SCE. Performance was higher than at the beginning of the experiment, confirming the improvement of the bioanode during the first 10-day period. The air-cathode i-E curves then showed the same trend as previously: the cathode firstly lost a part of its efficiency (day 18) and then stabilized (day 25).

The air-cathode was also replaced on an MFC equipped with a 50-cm^2 bioanode at day 18 (Fig. 3). Here again, the MFC performance immediately rose, reaching 3.12 mW. After a few days, the air-cathode tended to become biofouled and the power production decreased.

Air-cathode replacement was modelled numerically. The power curves were firstly modelled using the experimental i-E curves of the bioanode and the air cathode, which were recorded just before the cathode was changed. The numerical power curves overlapped the experimental data perfectly in all cases, without any parameter having to be adjusted, which demonstrated the validity of the model (Fig. 2 in Supplementary Data).

The model was then run in an identical way, but using the i-E curve of a clean air-cathode. The numerical power curves were close to the experimental curves that were recorded just after the air-cathode replacement. The experimental maximum powers were 1.99 and 3.12 mW for the MFCs equipped with a 9-cm^2 and a 50-cm^2 bioanode, respectively, while the model gave 1.84 and 3.19 mW. The model confirmed that the improvement of the cathode kinetics was responsible for the considerable improvement of the MFC performance. For the MFC equipped with the 9-cm^2

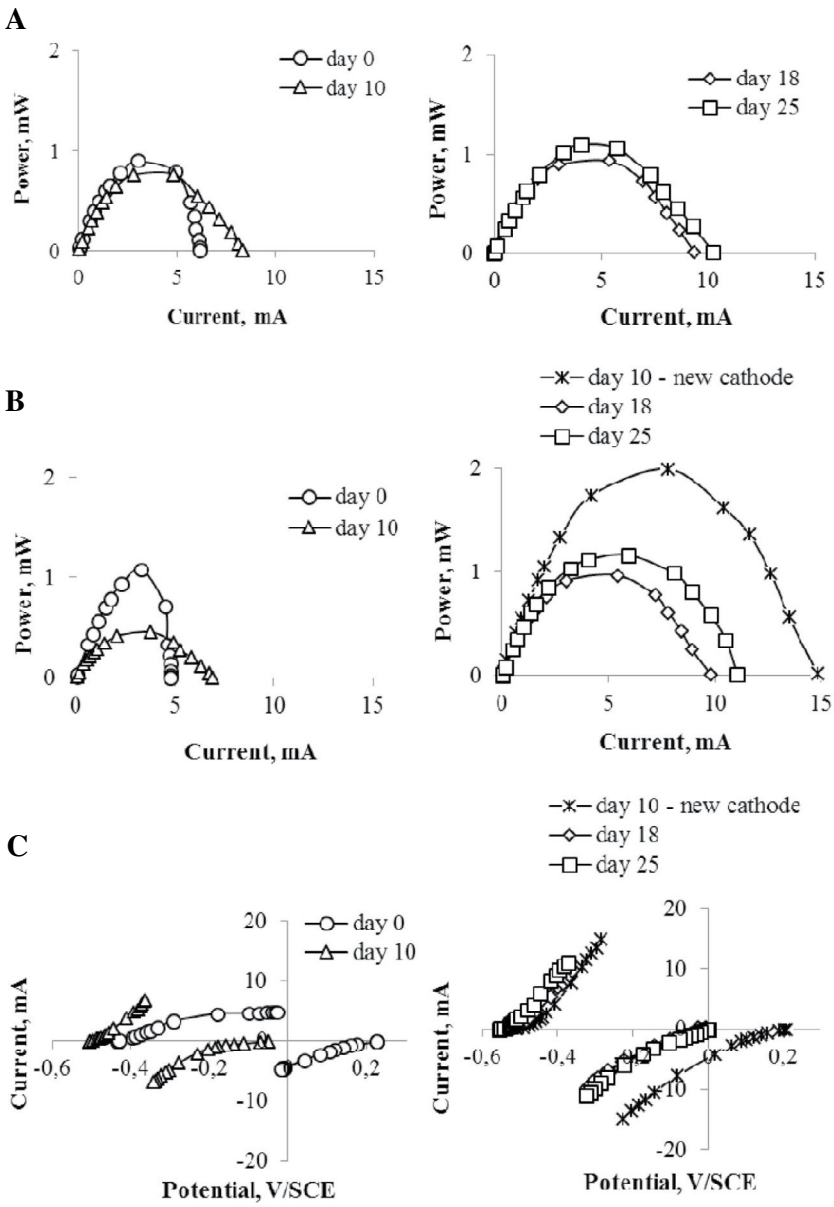

Fig. 2. Power curves in MFC operation with a 9-cm^2 bioanode, (A) the air-cathode was not changed; (B) duplicate with the air-cathode changed at day 10; (C) electrode kinetics (i-E curves) for the MFC characterized in (B) with the air-cathode changed at day 10.

bioanode, the slightly lower numerical value indicated a small improvement of the bioanode kinetics, which may have been due to the gentle movement of the electrolyte during cathode replacement. The perfect match between the experimental data and the numerical data obtained by just changing the air-cathode kinetics confirmed the suitability of the reactor design to enable the air-cathode to be changed without significantly disturbing the bioanode.

3.2. Discussion

Power densities were calculated with respect to the air-cathode surface area, which was equal to 15.9 cm^2 for each MFC. Before the air-cathode was changed, power densities around 0.6 and 0.7 W.m^{-2} were produced by the MFCs equipped with the 9-cm^2 and the 50-cm^2 bioanodes, respectively. The kinetics curves of the bioanodes and air-cathodes showed that the apparent power stability during the early days resulted from the concomitant cathode degradation and bioanode improvement. Actually, the bioanode improvement masked the degradation of the cathode kinetics during the starting period. After this period, the air-cathode ensured rather stable kinetics for several weeks.

Following these observations, it can be guessed that the maximum power that MFCs can produce may have been underestimated in numerous studies because the initial phase of air-cathode fouling is hard to detect considering the apparent stability of the power curves. Moreover, common MFC devices do not allow the air-cathode to be replaced without severely disturbing the system. Here, thanks to the removable-cathode design, replacing the air-cathode by a new one revealed the full potential of the MFCs. The new air cathodes boosted power density to 1.25 and 1.96 W.m^{-2} on the MFCs equipped with the 9-cm^2 and the 50-cm^2 bioanodes, respectively. This significant power boost confirms the considerable involvement of the initial air-cathode fouling in limiting the MFC performance.

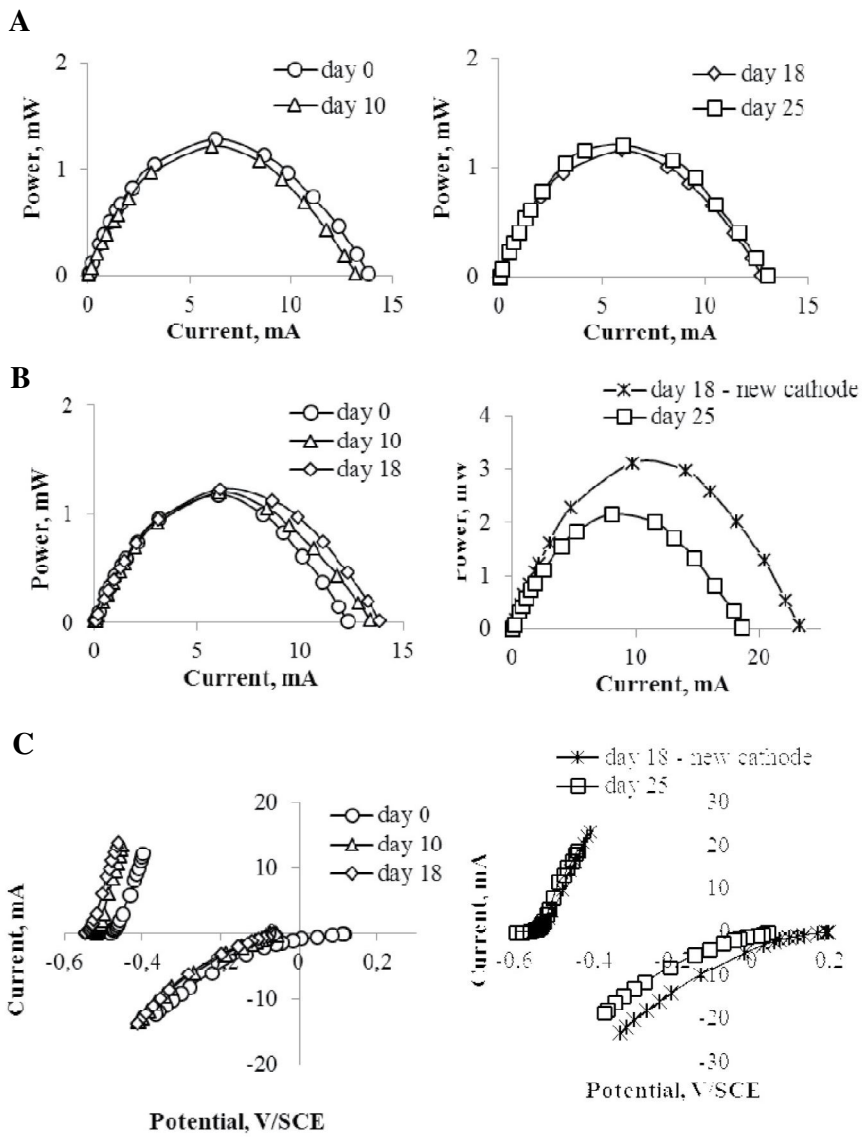

Fig. 3. Power curves of MFCs equipped with a 50-cm^2 bioanode, (A) the air-cathode was not changed; (B) duplicate with the air-cathode changed at day 18; (C) electrode kinetics (i-E curves) for the MFC characterized in (B) with the air-cathode changed at day 18.

The design of the reactor proved to be fully efficient and practical for replacing the air-cathode without altering MFC operation. Actually, it would not be economically sustainable to throw away the cathode when it was changed and cleaning procedures should now be considered. This new MFC design is a strong incentive to direct some research work towards the design of cleanable air-cathodes. This research direction started to be envisioned very recently (Pasternak et al., 2016) and the efficiency of the removable air-cathode MFC described here should arouse considerably increased interest in this new research objective.

4. Conclusion

Replacing the air-cathode during MFC operation evidenced the great importance of the initial biofouling of the air-cathode, which is generally hard to detect because it is masked by concomitant bioanode improvement. The fast initial biofouling of air-cathodes may consequently have been a widespread cause of underestimation of MFC performance so far. The efficiency of the removable air-cathode design described here now incites researchers to direct future work towards cleanable air-cathodes.

Acknowledgments

This work benefited from the support of the French state, managed by the Agence Nationale de la Recherche (ANR), within the framework of the Bioelec project (ANR-13-BIME-006).

Appendix A. Supplementary data

Supplementary data associated with this article can be found, in the online version, at http://dx.doi.org/10.1016/j.biortech.2016.09.095.

References

Ahn, Y., Zhang, F., Logan, B.E., 2014. Air humidity and water pressure effects on the performance of air-cathode microbial fuel cell cathodes. J. Power Sources 247, 655–659.

Cercado, B., Byrne, N., Bertrand, M., Pocaznoi, D., Rimboud, M., Achouak, W., Bergel, A., 2013. Garden compost inoculum leads to microbial bioanodes with potential-independent characteristics. Bioresour. Technol. 134, 276–284.

Chatterjee, P., Ghangrekar, M.M., 2014. Preparation of a fouling-resistant sustainable cathode for a single-chambered microbial fuel cell. Water Sci. Technol. 69, 634–639.

Lacroix, R., Da Silva, S., Viaplana Gaig, M., Rousseau, R., Delia, M.-L., Bergel, A., 2014. Modelling potential/current distribution in microbial electrochemical systems shows how the optimal bioanode architecture depends on electrolyte conductivity. PCCP 16, 22892–22902.
Li, N., Liu, Y., An, J., Feng, C., Wang, X., 2014. Bifunctional quaternary ammonium compounds to inhibit biofilm growth and enhance performance for activated carbon air-cathode in microbial fuel cells. J. Power Sources 272, 895–899.
Liu, W., Cheng, S., Sun, D., Huang, H., Chen, J., Cen, K., 2015. Inhibition of microbial growth on air cathodes of single chamber microbial fuel cells by incorporating enrofloxacin into the catalyst layer. Biosens. Bioelectron. 72, 44–50.
Ma, J., Wang, Z., Suor, D., Liu, S., Li, J., Wu, Z., 2014. Temporal variations of cathode performance in air-cathode single-chamber microbial fuel cells with different separators. J. Power Sources 272, 24–33.
Parot, S., Delia, M.-L., Bergel, A., 2008. Forming electrochemically active biofilms from garden compost under chronoamperometry. Bioresour. Technol. 99, 4809–4816.
Pasternak, G., Greenman, J., Ieropoulos, I., 2016. Regeneration of the power performance of cathodes affected by biofouling. Appl. Energy 173, 431–437.
Pocaznoi, D., Erable, B., Etcheverry, L., Delia, M.-L., Bergel, A., 2012. Towards an engineering-oriented strategy for building microbial anodes for microbial fuel cells. PCCP 14, 13332–13343.
Pu, L., Li, K., Chen, Z., Zhang, P., Zhang, X., Fu, Z., 2014. Silver electrodeposition on the activated carbon air cathode for performance improvement in microbial fuel cells. J. Power Sources 268, 476–481.
Rimboud, M., Pocaznoi, D., Erable, B., Bergel, A., 2014. Electroanalysis of microbial anodes for bioelectrochemical systems: basics, progress and perspectives. PCCP 16, 16349–16366.
Rismani-Yazdi, H., Carver, S.M., Christy, A.D., Tuovinen, I.H., 2008. Cathodic limitations in microbial fuel cells: an overview. J. Power Sources 180, 683–694.
Santini, M., Guilizzoni, M., Lorenzi, M., Atanassov, P., Marsili, E., Fest-Santini, S., Cristiani, P., Santoro, C., 2015. Three-dimensional X-ray microcomputed tomography of carbonates and biofilm on operated cathode in single chamber microbial fuel cell. Biointerphases 10, 031009.
Santoro, C., Cremins, M., Pasaogullari, U., Guilizzoni, M., Casalegno, A., Mackay, A., Li, B., 2013. Evaluation of water transport and oxygen presence in single chamber microbial fuel cells with carbon-based cathodes. J. Electrochem. Soc. 160, G3128–G3134.
Song, J., Liu, L., Yang, Q., Liu, J., Yu, T., Yang, F., Crittenden, J., 2015. PVDF layer as a separator on the solution-side of air-cathodes: the electricity generation, fouling and regeneration. RSC Adv. 5, 52361–52368.
Tlili, M.M., Benamor, M., Gabrielli, C., Perrot, H., Tribollet, B., 2003. Influence of the interfacial pH on electrochemical $CaCO_3$ precipitation. J. Electrochem. Soc. 150, C765–C771.
Wang, X., Feng, C., Ding, N., Zhang, Q., Li, N., Li, X., Zhang, Y., Zhou, Q., 2014. Accelerated OH- transport in activated carbon air cathode by modification of quaternary ammonium for microbial fuel cells. Environ. Sci. Technol. 48, 4191–4198.
Ye, Y., Zhu, X., Logan, B.E., 2016. Effect of buffer charge on performance of air-cathodes used in microbial fuel cells. Electrochem. Acta 194, 441–447.
Yuan, Y., Zhou, S., Tang, J., 2013. In situ investigation of cathode and local biofilm microenvironments reveals important roles of OH- and oxygen transport in microbial fuel cells. Environ. Sci. Technol. 47, 4911–4917.
Zhou, L., Fu, P., Cai, X., Zhou, S., Yuan, Y., 2016. Naturally derived carbon nanofibers as sustainable electrocatalysts for microbial energy harvesting: a new application of spider silk. Appl. Catal. B-Environ. 188, 31–38.